

# ACTIVATED CARBON: RECENT PROGRESS AND APPLICATIONS

## Abstract

Activated carbon has a larger surface area and well-developed porosity. It could be served as an absorbent to absorb unwanted materials. Synthesis of activated carbon is carried out via carbonization, physical activation, or chemical activation process. Precursors could be from agri-food industry wastes, municipal wastes, wood, and agricultural wastes. During the production of activated carbon, activating agent will be employed to develop porosity. Research findings indicated that an alkaline hydroxide was used for highly ordered (anthracites) while zinc chloride and phosphoric acid were employed for low-ordered precursors (lignocellulosic), respectively. Freundlich model and Langmuir isotherm were applied to multi-layer and mono-layer adsorption, respectively. In conclusion, the adsorption capacity (dyes, heavy metals, carbon dioxide and organic pollutants) was strongly depended onto experimental conditions.

**Keywords:** wastewater treatment; activated carbon; adsorption; water purification; industrial waste treatment.

## Author

### Ho Soonmin

Faculty of Health and Life Sciences,  
INTI International University, Putra Nilai,  
Negeri Sembilan, MALAYSIA  
soonmin.ho@newinti.edu.my

## I. INTRODUCTION

The population rise, significant increment in human activities and industrial growth resulted in environmental problems. Activated carbon has emerged as an excellent adsorbent in air purification and wastewater treatment process [1, 2]. The prepared activated carbon has excellent electrical conductivity, a larger surface area, high mechanical resistance behaviors, and tunable surface chemistry [3]. Generally, activated carbon can be synthesized using various carbonaceous materials such as municipal waste, waste from wood sector, waste from agri-food industry, industrial wastes [4], and fossil fuel wastes (Table 1). Table 2 highlights that precursor contained high carbon content and low ash content. During the preparation of activated carbon, activating agent will be used to create porosity [5, 6]. Alkaline hydroxide and zinc chloride & phosphoric acid were employed for highly ordered (anthracites) and low-ordered precursors (lignocellulosic), respectively. Heat transfer was conducted through conventional furnaces or microwave heating [7, 8]. Nitrogen and steam (figure 1) were used to transfer the heat to the solid sample and to eliminate evolved gaseous products [9, 10].

**Table 1: Starting Materials Employed In the Synthesis of Activated Carbons [4]**

<b>Agri-food industry wastes</b>	
Fibers	Banana, coconut, palm, jute
Processing paste	Vinegar must, oil, flaxseed, apple pulp, coffee
Seed husk	Rice, oat, cocoa, coffee, peanut, wheat
seeds	Palm, guava, orange, rapeseed
Soft shells	Orange, avocado, banana, pomegranate, watermelon, com, yucca
Nut shells	Hazelnut, almond, coconut, pistachio, walnut
Fruit pits	Apricot, olive, date, plum, peach, mango, avocado
<b>Wood and agricultural sector wastes</b>	
wood	Tree bark (palm, holm oak, olive, Acacia, pine, fir, eucalyptus)
Leaves and stems for harvesting	Tea, vine, kenaf, jute, tobacco, cane bagasse, com, cotton, sunflower, wheat, bamboo, hemp, esparto
<b>Municipal and industrial wastes</b>	
Waste materials (organic compounds)	Paper, tires, plastics, cardboard, waste from pulp and textile industry
Inorganic wastes	Steel industry sludge, sewage sludge
<b>Fossil fuel wastes</b>	
Coal	Lignite, peat, coal tar, fly ash, anthracite, subbituminous
Petroleum/oil	Coke, pitch

**Table 2: Ash Content, Elemental Analysis, and Lignocellulosic Composition of Different Types of Precursors [4]**

Precursor	Ultimate Analysis (wt %)				Lignocellulosic Composition (wt %)			Ash (wt %)
	C	H	O	N	Cellulose	Hemicellulose	Lignin	
Almond shell	49.5	6.3	44.0	0.2	32	26	25	2.2
Coconut shell	48.7	6.3	43.4	1.5	41	27	29	4.0
Palm shell	47.8	6.0	45.3	0.9	30	17	53	4.2
Hazelnut shell	47.0	6.5	46.0	1.0	25	28	42	1.4
Peanut shell	41.5	5.6	2.2	2.1	45	8	33	4.3
Palm kernel shell	43.6	4.9	51.6	0.5	30	21	47	2.4
Peach stone	45.9	6.1	47.4	0.6	46	14	33	1.5
Olive stone	45.0	5.8	48.3	0.2	32	33	30	2.1
Date pits	45.6	7.1	46.5	0.7	24	27	22	1.0
Orange peel	46.6	6.1	47.1	0.2	65	5	20	1.0
Tomato waste	59.0	8.2	29.8	0.3	33	24	35	1.6
Tobaco stalk	46.2	6.1	43.4	2.4	42	28	27	2.4
Cotton stalk	41.2	5.0	34.0	2.6	39	17	29	5.0
Corn stalk	45.5	6.2	41.1	0.8	23	43	16	7.5
Corn cob	46.3	5.6	42.2	0.6	43	37	15	3.5
Olive tree pruning	49.9	6.0	43.4	0.7	29	21	27	5.0
Vineyard pruning	47.6	5.6	41.1	1.8	38	34	27	3.5
Peach tree pruning	53.0	5.9	39.1	0.3	31	28	28	3.7
Oats straw	46.0	5.9	43.5	1.1	35	37	18	8.7
Sunflower straw	52.9	6.6	35.9	1.4	32	19	22	9.0
Barley straw	46.2	5.8	41.9	0.6	38	35	16	7.0
Rice straw	49.5	6.1	44.3	0.2	38	32	12	20.0
Wheat straw	42.7	5.6	39.7	0.3	33	20	15	3.7

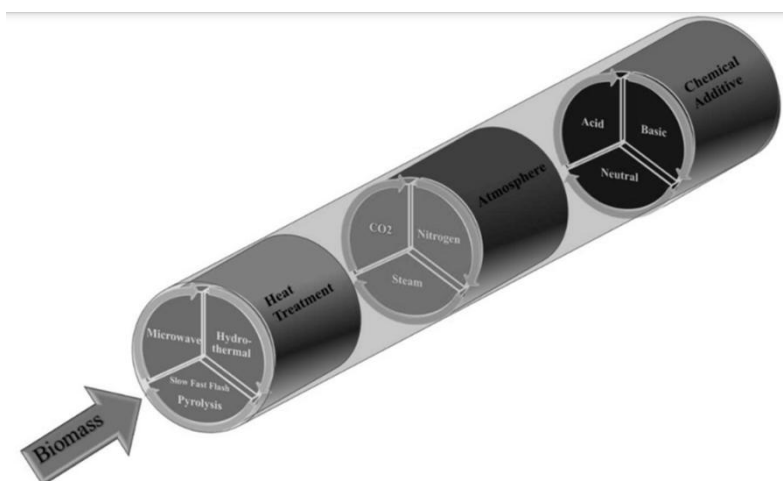


**Figure 1:** Experimental conditions involved in the synthesis of activated carbon [4]

In this book chapter, several types of precursors were used to synthesis activated carbon. The properties of the synthesized activated carbon were investigated using different techniques such as x-ray diffraction, scanning electron microscopy, Fourier Transform Infrared Spectroscopy, thermos gravimetry analysis and differential scanning calorimetry technique. Application of the prepared activated carbon has been reported.

## II. LITERATURE SURVEY

Marula fruits were found in Angola, Kenya, Malawi, Tanzania, Namibia, Botswana, Mozambique, and South Africa. In South Africa, these fruits were used to prepare Amarulaliquour due to the biggest producer in South Africa. Generally, trees could produce 500 kg fruits annually, and the fruit contained nuts (pale brown with oval shape). The nutshell consisted of moisture content of 5.5%, carbon content of 38.2% and ash content of 8.4%. Marula nutshell based activated carbon was synthesized via carbonization (200 °C to 600 °C) and activation process (phosphoric acid and sulphuric acid as activating agent). Table 3 shows the percentage of yield in different carbonization temperature and acid content [11]. It was noted that the yield increases when the concentration of activating agent was increased. Because of these activating agents digested amorphous lignin in the precursors. The presence of phosphoric acid and sulphuric acid inhibits the formation of tar and could reduce excessive sample burn-off. The untreated nutshell based activated carbon exhibited carbon content of 38.2%, pH of 5.5, moisture of 8.4%, ash content of 12.1%, bulk density of 0.64 g/cm<sup>3</sup>, and iodine number of 943.8 mg/g.

Table 4 indicates properties of the obtained activated carbon. Lower ash content could be observed using sulphuric acid solution during the treatment process, representing low particle density, and considered as excellent adsorbent. In the Fourier Transform Infrared Spectroscopy (FTIR) analysis, there are several peaks at 3400 cm<sup>-1</sup> (N-H group), 2950 cm<sup>-1</sup> (alkane), 1025 cm<sup>-1</sup> (anhydride group) could be detected in untreated nutshell activated carbon. When using 40% phosphoric acid, some bands could be found at 1550 cm<sup>-1</sup> (aliphatic carboxylic acid), 1200-1300 cm<sup>-1</sup> (nitrate group) and 1000 cm<sup>-1</sup> (phosphate group). Based on the thermogravimetry analysis (TGA) and differential scanning calorimetry (DSC) technique [12], weight loss occurred in several stages such as 195 °C (evaporation of water), 250 °C (degradation of hemicellulose and cellulose), and 370 °C (degradation of lignin). The influence of contact time (5 minutes=66%, 20 minutes=71%, 30 minutes=83%), pH (pH 2=removal is minimum, up to pH 6= significant increase, up to pH 10=slightly increase), adsorbent dosage (removal of dye is increases with increasing adsorbent dosage) and particle size (smaller size (less than 125 µm, resulted in higher adsorption) on the adsorption capacity was studied. Adsorption of methylene blue dye is endothermic (enthalpy= 15.24 kJ/mol) and spontaneous process (free energy=-31.51 to -34.49 kJ/mol).

Equilibrium data could be represented using Langmuir model ( $R^2=0.92-0.95$ , maximum adsorption capacity=28.25-33 mg/g). Pseudo second order kinetic isotherm ( $R^2$ =more than 0.999) best described the adsorption kinetic reaction if compared to pseudo first order kinetic model ( $R^2=0.79-0.95$ ) and Elovich model ( $R^2=0.87-0.91$ ). The effect of pH on the adsorption of metal ions has been reported [13] in Table 5. Percentage of adsorption increases [13] with increasing the pH (pH 4 to pH 6) because of the reduction in competition between hydrogen ions and metal ions (positive charged).

**Table 3: The Percentage Of Yield From Sulfuric Acid And Phosphoric Acid Treatment [11].**

Iphuric acid	Temperature (°C)			
	200	400	500	600
20 %	82.9%	15.6%	33.1%	39.8%
40 %	83.4%	19.8%	32.2%	40.6%
60 %	93.2%	28.5%	38%	41.5%
Phosphoric Acid				
20 %	73.6%	38.4%	45.1%	26.9%
40 %	77%	52.9%	67.9%	45.8%
60 %	68.4%	52.8%	66.6%	60.6%

**Table 4: The Physico-Chemical Characterization of The Prepared Activated Carbon [11].**

Temperature	Sulphuric acid content (%)	pH	Moisture (%)	Ash (%)	Bulk density (g/cm <sup>3</sup> )	Iodine value (mg/g)
200 °C	20	2.9	2.4	0.65	0.62	1036.1
	40	3.9	1.3	3.49	0.53	938.5
	60	2.4	10.7	0.97	0.54	947.4
400 °C	20	5.7	2.8	3.79	0.42	1036.1
	40	5.7	3.3	4.62	0.43	915.2
500 °C	60	6.1	2.5	4.53	0.45	990.8
Temperature	Phosphoric acid content					
200	60	2.8	6.4	14.2	0.54	1042.6
400	20	3.2	6.6	14.2	0.42	1048.3
500	40	2.7	14.6	29.8	0.82	1075.7
600	20	3.2	4.7	11.3	0.39	1131.9

**Table 5: Percentage Adsorption of Different Metal Ions onto Activated Carbon [13].**

Metal ion	pH 4	pH 5	pH 6
Pb <sup>2+</sup>	28.2	36.1	64.8
Zn <sup>2+</sup>	1.7	4.1	16.3
Cu <sup>2+</sup>	35.7	51.2	75.9
Ni <sup>2+</sup>	1.9	8.2	19.5
Fe <sup>2+</sup>	9.1	17.6	63.8
Mn <sup>2+</sup>	1.6	2.8	12.9
Hg <sup>2+</sup>	45.6	57.2	90.9
Cr <sup>3+</sup>	9.5	18	36
As <sup>3+</sup>	7.5	7	41.5
Cd <sup>2+</sup>	3.2	2.7	8.3

*Cordia Africana* is known as Wanza (in Ethiopia). This tree could be found in tropical Arabia and sub-Saharan Africa. It is heavily branched, grows about 4-15 meters tall. It produced fruits and its wood was employed for drums. Based on the scientific classification, order, family, genus, and species were identified as Boraginales, Boraginaceae, *Cordia* and *C. Africana* respectively. The leaves (as precursors) were washed with water to remove impurities [14], and grounded (125  $\mu\text{m}$  mesh size). Activation process was carried out in different temperatures (400  $^{\circ}\text{C}$  to 500  $^{\circ}\text{C}$ ) and concentrations of phosphoric acid (25% to 85%). The highest surface area (700  $\text{m}^2/\text{g}$ ) and yield (67%) could be obtained in the highlighted conditions (500  $^{\circ}\text{C}$  and concentration of 85%). Proximate analysis (moisture content=5.3%, bulk density=0.74  $\text{g}/\text{mL}$ , fixed carbon=64.3%, ash content=6.2%, and volatile matter=24.2%) of the prepared activated carbon was reported.

Scanning Electron Microscopy (SEM) images confirmed the dark structure (development of pores during the thermal and chemical activation). The highest chromium ( $\text{Cr}^{3+}$ ) ions removal was observed in the mentioned conditions (contact time=180 minutes, adsorbent dose=1.5g, initial concentration=0.6  $\text{g}/\text{L}$ , mixing speed=300 rpm). FTIR studies indicated different peaks were attributed to plenty of functional groups including hydroxyl group (3294  $\text{cm}^{-1}$ ), C-H stretching vibration (2990  $\text{cm}^{-1}$  and 2917  $\text{cm}^{-1}$ ), C=O stretching vibration (1716  $\text{cm}^{-1}$  and 1770  $\text{cm}^{-1}$ ), N-H stretching vibration (1620  $\text{cm}^{-1}$ , 1597  $\text{cm}^{-1}$ , 1543  $\text{cm}^{-1}$ ), C=C ring stretching (1405  $\text{cm}^{-1}$ ), C-O stretching vibration (1046  $\text{cm}^{-1}$ , 1022  $\text{cm}^{-1}$  and 1040  $\text{cm}^{-1}$ ), C-H bending vibration (855  $\text{cm}^{-1}$ , 879  $\text{cm}^{-1}$  and 873  $\text{cm}^{-1}$ ) and phosphate group (546  $\text{cm}^{-1}$  and 559  $\text{cm}^{-1}$ ). Heterogeneous adsorption occurred and supported by Freundlich model ( $R^2=0.88$ ). Pseudo first order kinetic model ( $R^2=0.99$ ) best fits with kinetic data, represented physisorption controls. In the regeneration investigations (figure 2), adsorption efficiency was dropped (86% to 17%) from the first cycle to seventh cycle due to some reasons such as adsorbent has changed its properties, loss of materials, and reduction of surface area. Sawdust was collected, sieved (50-60 mesh), dried, used for adsorption investigations [15].

Adsorption increases when the contact time was increased, achieved equilibrium (50 minutes for lead ion, and 70 minutes for nickel ion). It was noted that adsorption process is very low at more acidic pH value. However, gradually increases and finally reaches equilibrium (64% for lead ion, and 52% for nickel ion) at pH 7. Several polar functional groups (phenol, ketone, aldehyde, alcohol, amine, and carboxyl group) are protonated at low pH value. In contrast, when at higher pH value, the polar groups were deprotonated, and complexation with heavy metal ions. The best fit was reached with the Langmuir model based on the high correlation coefficient ( $R^2=\text{more than } 0.991$ ) value for the adsorption of lead ions (maximum adsorption capacity was 0.86 to 1.02  $\text{mmol}/\text{g}$ ) and nickel ions (maximum adsorption capacity was 1.78 to 2.1  $\text{mmol}/\text{g}$ ). In the thermodynamic studies, the free energy, enthalpy and entropy were found to be -11.35 to -13.38  $\text{kJ}/\text{mol.K}$ , 5.88  $\text{kJ}/\text{mol}$  & 0.0578  $\text{kJ}/\text{mol}$  and -8.03 to -9.89  $\text{kJ}/\text{mol.K}$ , 7.78  $\text{kJ}/\text{mol}$  & 0.0531  $\text{kJ}/\text{mol}$  for the removal of lead ions ( $\text{Pb}^{2+}$ ) and nickel ions ( $\text{Ni}^{2+}$ ), respectively.

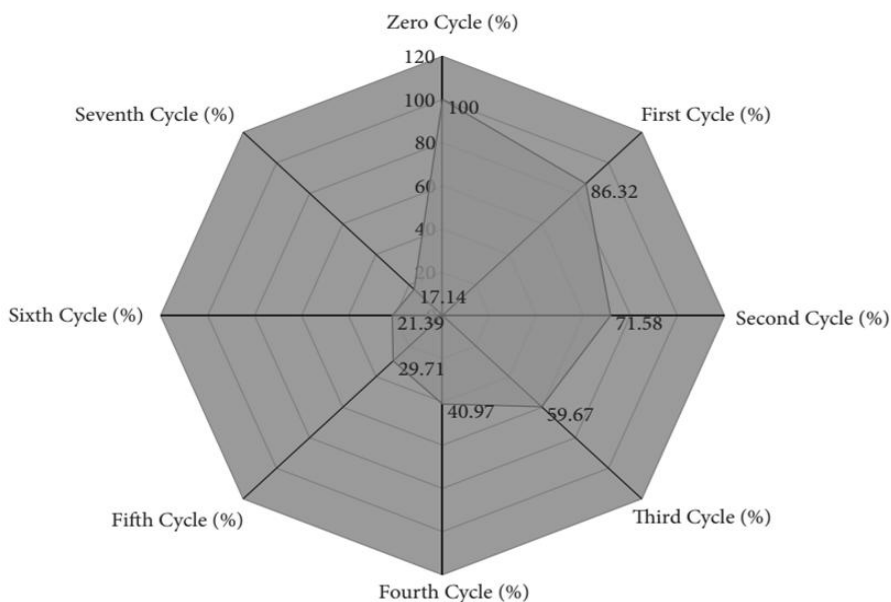


**Figure 2:** Regeneration study of used activated carbon [14].

The rice husk was placed in furnace [16], heated in specific conditions (residence time=1 hour, temperature =300 °C to 500 °C, and heating rate=20-25 °C/min) and was activated using phosphoric acid. Based on the response surface methodology, optimization of removal of phenol (efficiency of 97.16%) onto adsorbent has been highlighted (adsorbent dosage=4g, initial solute concentration=40.61 mg/L, and pretreatment temperature=441.46 °C). Raw materials have been treated with sodium hydroxide (NaOH) as reported by Joel and co-workers [17]. Physicochemical properties of the obtained active carbon have been described. It was noted that the percentage of yield, carbon content, volatile matter and moisture content reduce when the carbonization temperature (promoted carbon burn-off) and impregnation ratio (promoted the release of volatiles) were increased. The point of zero charges (pHpzc) was 6.8 and showed wide opening pores with mesoporous surface area based on the x-ray diffraction (XRD) and SEM analysis. FTIR studies confirmed the presence of carbonyl ( $2336\text{ cm}^{-1}$  to  $2376\text{ cm}^{-1}$ ), hydroxyl ( $3743\text{ cm}^{-1}$  to  $3646\text{ cm}^{-1}$ ), aromatic ( $1400\text{ cm}^{-1}$  and  $1673\text{ cm}^{-1}$ ) and amine groups ( $148\text{ cm}^{-1}$ ), good for adsorption process. The study has highlighted ammonia and gasoline could be removed using these activated carbons. Rice husk was collected from Bangladesh, and the chemical activation was carried out using zinc chloride solution as proposed by Arifur and co-workers [18]. The surface area ( $681\text{ m}^2/\text{g}$ ), yield (36%), ash content (3%), mean pore radius (2.42 nm), total pore volume ( $0.42\text{ cm}^3/\text{g}$ ), moisture content (4.28%), and bulk density ( $0.84\text{ g/mL}$ ) were reported. The highest adsorption percentage was 97.15% in the optimized conditions (initial concentration of methylene blue=4mg/L, flow rate=1.4mL/min, particle size=140  $\mu\text{m}$ , pH=10, and initial volume of methylene blue=50 mL). Crystal violet dye was removed from wastewater using xanthated rice husk based activated carbon [19]. XRD studies showed amorphous structure (high content of cellulose, lignin, and hemicellulose), let the dye compounds penetrate the surface rapidly. Elemental analysis indicated a higher sulfur percentage in xanthated rice husk (5.31%) if compared to raw (0.24%) and charred rice husk (1.8%). Based on the FTIR investigations, several functional groups (C=O, NH, CH, C-O and OH) take part in the adsorption process. Correlation coefficient ( $R^2$ ) was observed to be higher if compared to

Freundlich model in charred rice husk ( $R^2=0.9934$ , maximum adsorption capacity=62.85 mg/g) and xanthated rice husk ( $R^2=0.9958$ , maximum adsorption capacity=90.02 mg/g). In the adsorption kinetic studies, the dye ion was chemisorbed to xanthated rice husk ( $R^2=0.9981$ ) and charred rice husk ( $R^2=0.9974$ ), followed pseudo second order kinetic model.

Wheat straw is defined as stalk left after wheat grains were harvested by the farmers. It was considered a waste and farmers will burn it (created air pollution). Wheat straw based activated carbon [20] was produced through carbonization (flow rate=350 cm<sup>3</sup>/min, time=120 minutes, temperature=300 °C, atmosphere=nitrogen gas) and activation process (temperature=800 °C, time=60 minutes, heating rate=10 °C/min, activating agent=KOH). Properties of the wheat straw such as carbon content (44.82%), hydrogen content (7.32%), nitrogen content (1.5%), volatile matter (86.7%), ash content (10.41%), moisture content (7.12%), lignin (18.4%), cellulose (37.5%), and hemicellulose (27.8%) were reported. The DTG analysis (figure 3) showed three stages at temperature below 100 °C (drying stage), over 200 °C (emission of volatiles), and over 300 °C (lignin decomposition).

As shown in the SEM images, cavities could be seen during the activation process, enhanced the porosity formation. The volume of micropores (0.48 cm<sup>3</sup>/g), surface area (1164 m<sup>2</sup>/g), acidic group concentration (8712 meq/g), basic group concentration (3631 meq/g) and the pH of point of zero charge (pH 5.99) were described. In the adsorption studies, the second order kinetic isotherm and Langmuir model (maximum adsorption capacity was 264.9 mg/g) fitted the data better if compared to other models. The presence of sodium chloride had no influence on the adsorption of diphenolic acid removal, favored adsorbent-adsorbate dispersive interactions (via screening effect). The properties of diphenolic acid have been described in Table 6. Microporous activated carbon was produced using KOH and through microwave heating [21]. Total pore volume, surface area, micropores were 0.6 cm<sup>3</sup>/g, 1250 m<sup>2</sup>/g, and 76%, respectively in the specific conditions (less than 30 minutes, at 600 W, KOH/char ratio of 3). Adsorption data (toluene and acetone) were fitted using Dubinin-Radushkevich model. Wheat straw was collected from Hebai (China), sieved (100 to 140 mesh), activated with zinc chloride and potassium hydroxide [22]. Activated carbon treated with zinc chloride had higher surface area (Table 7), more micropores and aromatic structure.

XRD data confirmed zinc chloride treated carbon has more orderly structure, diffraction peak has been moved from 19.07 ° (potassium hydroxide treated) to 22.18 ° (zinc chloride treated). According to SEM images, different morphology could be observed in zinc chloride (uniform surface, well-developed with many circular pores) and potassium hydroxide (rough surface, big pores on it) treated carbons. Based on the Langmuir model, maximum adsorption capacity values of methylene blue dyes were 265.96 mg/g and 146.84 mg/g in ZnCl<sub>2</sub> ( $R^2=0.9935$ ) and KOH ( $R^2=0.9978$ ) treated activated carbon, respectively. In the adsorption kinetics, pseudo second order kinetic isotherm ( $R^2=0.9994$ ) fitted the data better if compared to Elovich ( $R^2=0.9781$ ) and pseudo first order model ( $R^2=0.9803$ ), represented chemisorption happened during the adsorption process. High correlation coefficient value in Weber and Morris model ( $R^2=0.9901$ ), indicating intraparticle diffusion happened. In the regeneration studies (using thermal treatment), we found that regeneration efficacy reduced when the regeneration cycle was increased (collapse of porous structure). However, we can observe that regeneration efficiency successfully remained more than 70% (even after five cycles).

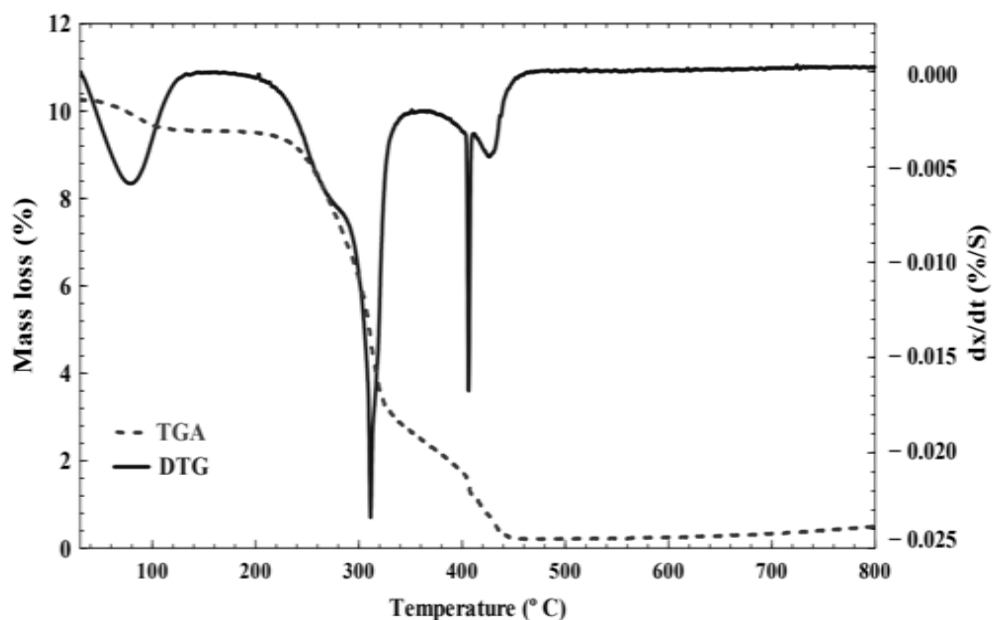


**Figure 3:** Thermogravimetric analysis (TGA/DTG) for wheat straw based activated carbon [20].

**Table 6: Properties of Diphenolic Acid**

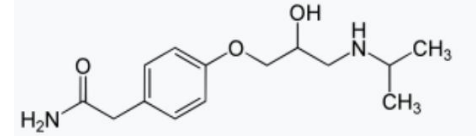
Chemical formula	$C_{17}H_{18}O_4$
Molar mass	286.33 g/mol
Melting point	168 °C to 171 °C
Boiling point	507 °C
Flash point	208 °C
Color	White
Density	1.07 g/cm <sup>3</sup>
Solubility	Soluble (acetone, ethanol, isopropanol, acetic acid), insoluble (carbon tetrachloride, benzene, xylene)
Structure	

**Table 7: Properties of Activated Carbon Produced Through Zinc Chloride And Potassium Hydroxide Activation Process [22]**

	Zinc chloride treated activated carbon	Potassium hydroxide treated activated carbon
Surface area (m <sup>2</sup> /g)	907	552
Total pore volume (cm <sup>3</sup> /g)	0.511	0.387
Yield (%)	37.45	26.19
Diameter average (nm)	2.25	2.8
Micro pore volume (cm <sup>3</sup> /g)	0.375	0.227
Mesopore volume (cm <sup>3</sup> /g)	0.148	0.15

*Stipa tenacissima* grows in rocky, dry, and base rich soils. This steppe-like grassland could be found in several countries (Algeria, Portugal, Morocco, Tunisia, Libya, France, and Spain). Based on the scientific classification, order, family, subfamily, genus, and species were identified as Poales, Poaceae, Pooideae, *Stipa* and *S. tenacissima*, respectively. Chemical activation of *Stipa tenacissima* leaves (from Southern Algeria) based activated carbon using activating agent (phosphoric acid) was reported [23]. Proximate analysis of leaves such as ash content (1.19%), volatile matter (62.81%), fixed carbon content (24.5%) and moisture content (11.5%) were reported. Carbon content (76.46% to 91.04%) increased, but hydrogen (2.43% to 1.57%) and oxygen content (18.56% to 6.99%) reduced with an increasing of the temperature (400 °C to 600 °C) and the impregnation ratio of 1. In the adsorption studies, the Langmuir model (maximum adsorption capacity = 98.65 to 169.69 mg/g) fitted the data better if compared to Freundlich model ( $R^2=0.91$  to 0.98) and Temkin isotherm ( $R^2=0.81$  to 0.83). The adsorption kinetic of atenolol on the adsorbent could be described using pseudo second order model ( $R^2=0.999$ ). The  $pH_{pzc}$  was observed to be pH 8, and prepared adsorbent showed negative charged (rich in oxygenated groups). As highlighted in the mechanism of atenolol adsorption, the atenolol was fixed through the interaction H-H and H-O groups (figure 4). Atenolol is used to treat irregular heartbeats, high blood pressure and chess pain. It is beta blocker medication, taken by injection or by mouth. Properties and pharmacokinetic data of atenolol have been reported (Table 8). Activated carbon (surface area was 1125 m<sup>2</sup>/g) was synthesized [24] using chemical activation (phosphoric acid) in specific conditions (holding time of 60 minutes, ratio of activating agent to starting material was 3:1). In thermodynamic studies, adsorption of heavy metal ions is an endothermic and spontaneous reaction. Low-cost material such as *stipa tenacissima* fibers (collect from Boussaada, Algiers) was used to remove methylene blue dye [25]. Mesoporous structure was well-developed and surface area was 62.48 m<sup>2</sup>/g. Equilibrium was observed after 40 minutes (at 30 °C, adsorbent dosage=5 g/L). Experimental data was supported by Freundlich model ( $R^2=0.923$ ) and pseudo second order model ( $R^2=1$ ). According to thermodynamic analysis, adsorption of methylene blue was exothermic process (enthalpy=-11.318 kJ/mol) and spontaneous (free energy=-10.146 kJ/mol).

**Table 8: Properties and Pharmacokinetic Data of Atenolol**

Structure	
Formula	C <sub>14</sub> H <sub>22</sub> N <sub>2</sub> O <sub>3</sub>
Molar mass	266.34 g/mol
Bioavailability	40-50%
Protein binding	6-16%
Metabolism	Liver<10%
Elimination half-life	6-7 hours
Excretion	Kidney

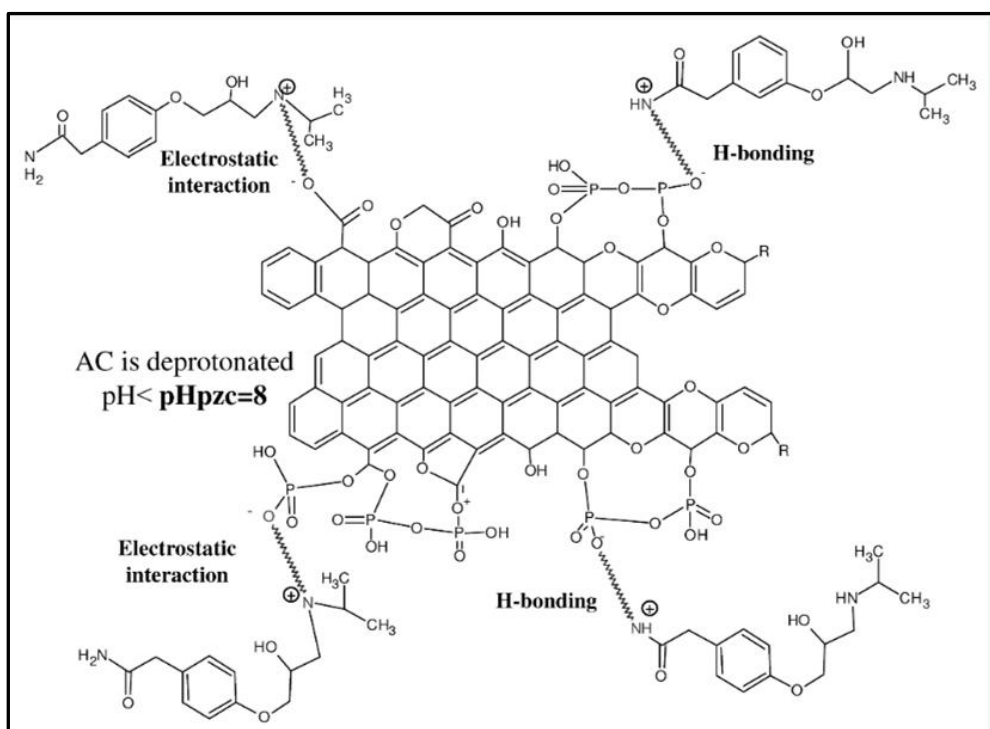


**Figure 4:** Adsorption of mechanism of atenolol on the *Stipa tenacissima* leaves based activated carbon [23]

Dragon fruit is known as pitaya and is available everywhere. The fruit has white flesh with small black seed (inside) and pink oval (outside). It is fat-free fruit, has very low calories and high amount of fiber. Dragon fruit skin was considered a waste (no economic value). Removal of methylene blue dye has been reported using dragon fruit skin based activated carbon [26]. Adsorption equilibrium was reached within 60 minutes. Langmuir isotherm type II ( $R^2=0.972$ ) and pseudo second order model ( $R^2=0.996$ ) represented adsorption data. Several functional groups such as aromatic vibration ( $891\text{ cm}^{-1}$ ), C=C ( $1643\text{ cm}^{-1}$ ), C=O ( $1730\text{ cm}^{-1}$ ), OH ( $3423\text{ cm}^{-1}$ ), and C-N ( $1326\text{ cm}^{-1}$ ) could be observed in the obtained

activated carbon [27]. SEM images confirmed that rough morphology and irregular surface could be seen before the adsorption process. However, the surface of the adsorbent has been covered with dye after the adsorption process. Removal of Congo Red onto activated carbon is rapid (90% dye removal), reached equilibrium within 30 minutes. Activated carbon performed better in the presence of sodium chloride due to the screening effects. The Sips model (adsorption capacity=71.7 mg/g) could be used to explain the adsorption of dye onto adsorbent. The Pseudo-second order model with  $R^2$ =more than 0.9735, obeyed the adsorption kinetics. *Hylocereus polyrhizus* was sieved (100 to 230 mesh), used to prepare activated carbon. The amount of copper (II) ions absorbed is 5.001mg/g (5 minutes), 5.27 mg/g (10 minutes), then decreases (30 minutes to 90 minutes) due to the active site saturated. At low pH (pH 2, adsorbed amount=0.72 mg/g). There are several precursors (Table 9) such as the *Delonix regia* pods, Coal gasification fine slag, *Prosopis Juliflora* plant, Acai, Brazil nut, oil palm shell, Babassu, mango seeds, waste tea, banana, grape, watermelon, cocoa, bamboo, and black cumin seed, have been used to prepare activated carbon. The obtained adsorbent has been studied by using FTIR, TGA, DTG, EDX, SEM, EDX.

**Table 9: Textural properties and porosity characteristics of activated carbon**

Raw materials	Results	References
Delonix regia pods	<ul style="list-style-type: none"> <li>Biomass waste based activated carbon (solvated polystyrene-based binders) showed mesoporous porosity [28], pore size of 2.45 nm and surface area of 314.9 m<sup>2</sup>/g.</li> </ul>	Adewale et al., 2023
Coal gasification fine slag	<ul style="list-style-type: none"> <li>Carbon content was 33.61% for the activated carbon synthesized in low temperature air activation [29].</li> <li>Pore volume and specific surface area increased 7.8% and 21.5%, respectively in the best conditions.</li> <li>The highest removal of carbon dioxide reached 21.03 cm<sup>3</sup>/g.</li> <li>FTIR: Removal of hydrocarbon could be observed in pores</li> </ul>	Zheng et al., 2023
<i>Prosopis Juliflora</i> plant (stem)	<ul style="list-style-type: none"> <li>Surface area is 252.73 m<sup>2</sup>/g in the specific conditions (chemical activation, in muffle furnace, impregnation ratio of 1:0.5, temperature of 800 °C, activation agent is zinc chloride, activation time=1 hour).</li> <li>Langmuir model and pseudo-second-order kinetic isotherm represented adsorption data (methylene blue).</li> <li>More negative free energy could be observed in thermodynamic analysis [30].</li> </ul>	Vasiraja et al., 2023
Acai, Brazil nut, oil	<ul style="list-style-type: none"> <li>Surface area, total pore volume and</li> </ul>	Joao et al., 2023

palm shell, Babassu	<p>average pore diameter were studied using Acai (703 m<sup>2</sup>/g, 0.35 cm<sup>3</sup>/g, 2.04 nm), Brazil nut (911 m<sup>2</sup>/g, 0.45 cm<sup>3</sup>/g, 2.05 nm), oil palm shell (569 m<sup>2</sup>/g, 0.27 cm<sup>3</sup>/g, 2 nm), Babassu (1101 m<sup>2</sup>/g, 0.51 cm<sup>3</sup>/g, 1.94 nm).</p> <ul style="list-style-type: none"> <li>• The highest capacity (phenol) reached 596.69 mg/g in babassu based activated carbon.</li> <li>• Freundlich model represented adsorption data [31].</li> <li>• EDX: Higher carbon content in activated carbon, while less oxygen and hydrogen content (if compared to precursors).</li> </ul>	
Mango seeds	<ul style="list-style-type: none"> <li>• Several types of functional groups (carboxylic acid, alkyl halide, amines, aromatics, alkene, ethers, ketones, and phosphine oxide) have been identified in mangoseed based activated carbon [32].</li> <li>• The highest removal efficiency was 94.01% in highlighted conditions (contact time=64 minutes, adsorbent mass=1.95g, initial concentration of paracetamol=150 ppm).</li> <li>• High correlation coefficient in Freundlich model (R<sup>2</sup>=0.9718) and pseudo first order kinetic model (R<sup>2</sup>=0.9435).</li> </ul>	Preglo et al., 2023
Banana peduncle	<ul style="list-style-type: none"> <li>• The highest As(V) and Cr(VI) removal were found to be 79.32% and 69.73% in virgin banana peduncle based activated carbon [33].</li> <li>• The highest As(V) and Cr(VI) removal were found to be 69.08% and 73.78% in iron-impregnated banana peduncle based activated carbon.</li> <li>• Adsorption process is an endothermic process, followed pseudo-second order reaction.</li> <li>• BET: 749.7 m<sup>2</sup>/g (virgin activated carbon), 369.7 m<sup>2</sup>/g (iron-impregnated activated carbon)</li> <li>• Pore volume: 0.455 cm<sup>3</sup>/g (virgin activated carbon), 0.322 cm<sup>3</sup>/g (iron-impregnated activated carbon)</li> </ul>	Zobia et al., 2023

Watermelon peel	<ul style="list-style-type: none"> <li>• Mesoporous watermelon based activated carbon has been synthesized through microwave assisted <math>K_2CO_3</math> activation process [34].</li> <li>• The highest removal of methylene blue dye reached 50 mg/L (adsorbent dose=0.056g, contact time=4.4 minutes, working temperature=39 °C, pH=8.4).</li> <li>• The adsorption process was endothermic reaction, best fitness to the Langmuir model (capacity of 312.8 mg/g) and pseudo second order kinetic model.</li> </ul>	Tarek et al., 2023
Grape marc	<ul style="list-style-type: none"> <li>• Based on the thermodynamic studies, <math>\Delta G</math> less than 0, <math>\Delta H=12.28</math> kJ/mol, <math>\Delta S=0.041</math>kJ/mol.K.</li> <li>• The adsorption capacity (azo dye (AO7)) increases when the temperature was increased from 25 °C (140.5 mg/g) to 55 °C (174.6 mg/g).</li> <li>• FTIR: ethanol is bound to prepared carbon [35].</li> </ul>	Bourahla et al., 2023
Bamboo	<ul style="list-style-type: none"> <li>• Higher percentage of yield could be seen in the bamboo based activated carbon (<math>FeCl_2</math> activation, one-pot pyrolysis) if compared to steam and KOH activation method [36].</li> <li>• The largest surface area (<math>1290.9</math> m<sup>2</sup>/g) and pore volume (<math>0.67</math> m<sup>3</sup>/g) could be observed when the activation temperature was 900 °C.</li> <li>• The highest adsorption capacity (hexavalent chromium ions) reached 13.65 mg/g, and strongly affected by the pore configuration.</li> <li>• Nitrogen adsorption-desorption: many pores were produced with increasing the activation temperature (700 °C to 900 °C).</li> </ul>	Meijuan et al., 2022
Cocoa pod husk	<ul style="list-style-type: none"> <li>• Adsorption (2,4-dichlorophenol) data could be represented using pseudo-second order model and Langmuir isotherm [37].</li> <li>• According to the thermodynamic studies, <math>\Delta G</math> and <math>\Delta S</math> were -35.287 kJ/mol and +0.335 kJ/mol.K, respectively.</li> <li>• Physisorption reaction was observed, and the Arrhenius constant value (&lt;100</li> </ul>	Victor et al., 2023

	kJ/mol).	
Black cumin (Nigella sativa) seed pulp	<ul style="list-style-type: none"> <li>• Thermodynamics data revealed that entropy of system was reduced, it was exothermic process and spontaneous reaction [38].</li> <li>• The highest adsorption capacity (basic yellow 28) reached 212 mg/g on black seed based activated carbon according to Langmuir curves.</li> <li>• The highest adsorption capacity (methylene violet 2B) achieved 164 mg/g on black seed based activated carbon according to Langmuir curves.</li> <li>• TGA: evaporation of moisture (up to 135 °C), decomposition of lignin, hemicellulose, cellulose (until 600 °C).</li> </ul>	Sedef et al., 2023
Waste tea (Camellia sinensis)	<ul style="list-style-type: none"> <li>• Bulk density (0.3 g/mL), ash content (3.4%), volatile matter (26.76%) and moisture content (4.34%) were reported for the activated carbon produced using 30% sulfuric acid [39].</li> <li>• Based on the research findings, 100% removal of cadmium ions (concentration of cadmium was 0.5 mg/L and 1 mg/L) in this activated carbon.</li> <li>• More methylene blue has been removed when the concentration of sulfuric acid increased due to surface area was increased.</li> <li>• XRD: Broad peak has been seen (<math>2\theta=14-22^\circ</math>), representing amorphous materials.</li> <li>• SEM: Different morphologies could be observed using 5% (porous structure), 10% (honeycomb like pore) and 20% (macropore in size) sulphuric acid solution.</li> </ul>	Affandy et al., 2023

### III. CONCLUSIONS

Currently, several agricultural, industrial, municipal and food wastes have been used to synthesis activated carbon. This activated carbon could be used to removal contaminant or unwanted materials through adsorption process. The prepared activated carbon has a larger surface area and well-developed porosity. Experimental results showed that alkaline hydroxide was used for highly ordered (anthracites) while zinc chloride and phosphoric acid were employed for low-ordered precursors (lignocellulosic), respectively. The multi-layer and mono-layer adsorption could be represented using Freundlich model and Langmuir

isotherm respectively. The removal efficiency (dyes, heavy metals, carbon dioxide and organic pollutants) was strongly depended onto experimental conditions.

#### IV. ACKNOWLEDGEMENT

This research work was supported by INTI INTERNATIONAL UNIVERSITY.

#### REFERENCES

- [1] K. Malini, D. Selvakumar, and N. Kumar, "Activated carbon from biomass: Preparation, factors improving basicity and surface properties for enhanced CO<sub>2</sub> capture capacity – A review," *Journal of CO<sub>2</sub> Utilization*, <https://doi.org/10.1016/j.jcou.2022.102318>, 2023.
- [2] M. Hossain, D. Islam, and A. Rahaman, "Production of cost-effective activated carbon from tea waste for tannery wastewater treatment," *Applied Water Science*, <https://doi.org/10.1007/s13201-023-01879-5>, 2023.
- [3] S.M. Ho, and M. Saad, "Review on heavy metal and dye removal via activated carbon adsorption process," *Asian Journal of Chemistry*, vol. 35, pp. 1-16, 2023.
- [4] J. Alcañiz, M. Román, and A. Lillo, "Chemical Activation of Lignocellulosic Precursors and Residues: What Else to Consider?" *Molecules*, <https://doi.org/10.3390/molecules27051630>, 2022.
- [5] T. Maryam, A. Babak, C. Pevida, and I. Milad, "Development of novel waste tea-derived activated carbon promoted with SiO<sub>2</sub> nanoparticles as highly robust and easily fluidizable sorbent for low-temperature CO<sub>2</sub> capture," *Journal of Environmental Chemical Engineering*, <https://doi.org/10.1016/j.jece.2023.110437>, 2023.
- [6] S.M. Ho, "Low-Cost Adsorbents for the Removal of Phenol/Phenolics, Pesticides, and Dyes from Wastewater Systems: A Review," *Water*, <https://doi.org/10.3390/w14203203>, 2022
- [7] N. Hasdi, N. Ahmad, and W. Siti, "An Overview of Activated Carbon Preparation from Various Precursors," *Scientific Research Journal*, vol. 20, pp. 51-87, 2023.
- [8] S.M. Ho, "A Review of Chemical Activating Agent on the Properties of Activated Carbon," *International Journal of Chemistry and Research*, vol. S1, pp. 1-13.
- [9] G. Alam, T. Ahmad, H. Abdul, and M. Danish, "Response surface methodology approach of phenol removal study using high-quality activated carbon derived from H<sub>3</sub>PO<sub>4</sub> activation of Acacia mangium wood," *Diamond and Related Materials*, <https://doi.org/10.1016/j.diamond.2022.109632>, 2023.
- [10] S.M. Ho, and A. Nassereldeen, "Review On Activated Carbon: Synthesis, Properties And Applications," *International Journal of Engineering Trends and Technology*, vol. 69, pp. 124-139, 2021.
- [11] M. Tafadzwa, M. Shepherd, C. Armistice, and S. Munyaradzi, "Synthesis and Characterization of Activated Carbon Obtained from Marula (*Sclerocarya birrea*) Nutshell," *Journal of Chemistry*, <https://doi.org/10.1155/2021/5552224>, 2021.
- [12] N. Joshua, S. Stanley and O. John, "Characterization of pulverized Marula seed husk and its potential for the sequestration of methylene blue from aqueous solution," *BMC Chemistry*, <https://doi.org/10.1186/s13065-019-0530-x>, 2019.
- [13] M. Jane, A. Tanya, I. Ncube and J. Colin, "Adsorption of heavy metals by agroforestry waste derived activated carbons applied to aqueous solutions," *African Journal of Biotechnology*, vol. 13, pp. 1579-1587, 2014.
- [14] K. Estifanos, F. Jemal, T. Solomon, and T. Thabo, "The Application of the Activated Carbon from *Cordia africana* Leaves for Adsorption of Chromium (III) from an Aqueous Solution," *Journal of Chemistry*, <https://doi.org/10.1155/2022/4874502>, 2022.
- [15] M. Syed, "Sawdust of lam tree (*Cordia africana*) as a low-cost, sustainable and easily available adsorbent for the removal of toxic metals like Pb(II) and Ni(II) from aqueous solution," *European Journal of Wood and Wood Products*, vol. 69, pp. 75–83, 2011.
- [16] Y. Mohammad, E. Shaibu, A. Giwa, and A. Okuofu, "Modeling and Optimization for Production of Rice Husk Activated Carbon and Adsorption of Phenol." *Journal of Engineering*, <http://dx.doi.org/10.1155/2014/278075>, 2014.
- [17] E. Vunain, and B. Timothy, "Synthesis and Characterization of Activated Carbons Prepared from Agro-Wastes by Chemical Activation," *Journal of Chemistry*, <https://doi.org/10.1155/2022/9975444>, 2022.
- [18] M. Arifur, A. Ruhul, and A. Alam, "Removal of Methylene Blue from Wastewater Using Activated Carbon Prepared from Rice Husk," *Dhaka University Journal of Science*, vol. 60, pp. 185-189, 2012.

- [19] L. Puspa, R. Poudel, P. Sujana, and B. Ajaya, "Adsorption and removal of crystal violet dye from aqueous solution by modified rice husk," *Heliyon*, <https://doi.org/10.1016/j.heliyon.2022.e09261>, 2022.
- [20] R. Alrowais, N. Said, T. Bashir, and A. Ghazy, "Adsorption of Diphenolic Acid from Contaminated Water onto Commercial and Prepared Activated Carbons from Wheat Straw," *Water*, <https://doi.org/10.3390/w15030555>, 2023.
- [21] H. Mao, D. Zhou, H. Zaher, and S. Wang, "Microporous activated carbon from pinewood and wheat straw by microwave-assisted KOH treatment for the adsorption of toluene and acetone vapors. *RSC Advances*, vol. 5, pp. 36051-36058, 2015.
- [22] Y. Ma, "Comparison of Activated Carbons Prepared from Wheat Straw via  $ZnCl_2$  and KOH Activation," *Waste and Biomass Valorization*, vol. 8, pp. 549–559 (2017).
- [23] N. Madani, V. Jose, C. Ouiza, and B. Naima, "Activated Carbon from *Stipa tenacissima* for the Adsorption of Atenolol," *Journal of Carbon Research*, <https://doi.org/10.3390/c8040066>, 2022.
- [24] N. Madani, O. Bouchenafa, J. Mohammedi, and D. Varela, "Removal of heavy metal ions by adsorption onto activated carbon prepared from *Stipa tenacissima* leaves," *Desalination and Water Treatment*, vol.64, pp. 179-188, 2017.
- [25] S. Hemsas, and M. Hachemi, "Adsorption of methylene blue dye by *stipa tenacissima* L. (Alfa fibers) in aqueous solution: equilibrium, thermodynamics, kinetic mechanism," *Revue Roumaine de Chimie*, vol. 64, pp. 775-784, 2019.
- [26] N. Priyantha, B.Lim, and K. Dahri, "Dragon fruit skin as a potential biosorbent for the removal of methylene blue dye from aqueous solution," *International Food Research Journal*, vol.22, pp. 2141-2148, 2015.
- [27] B. Linda, P. Namal, A. Siti, and Y. Lu, "Sequestration of toxic Congo red dye through the utilization of red dragon fruit peel: linear versus nonlinear regression analyses of isotherm and kinetics," *Desalination and Water treatment*, vol. 218, pp. 409-422, 2021.
- [28] A. Adewale, O. Kayode, C. Ebuka, and M. Ndagi, "Preparation of activated carbon monolith from waste biomass using solvated polystyrene-based binder," *Advances in Materials and Processing Technologies*, <https://doi.org/10.1080/2374068X.2023.2189679>, 2023.
- [29] G. Zheng, X. Han, J. Wang, and C. Zhang, "Preparation of activated carbon adsorption materials derived from coal gasification fine slag via low-temperature air activation," *Gas Science and Engineering*, <https://doi.org/10.1016/j.jgsce.2023.205069>, 2023.
- [30] N. Vasiraja, A. Joshua, and R. Sathiya, "Preparation and Physio-Chemical characterisation of activated carbon derived from *Prosopis juliflora* stem for the removal of methylene blue dye and heavy metal containing textile industry effluent," *Journal of Cleaner Production*, <https://doi.org/10.1016/j.jclepro.2023.136579>, 2023.
- [31] R. Joao, S. Leandro, A. Luis, and Z. Jose, "Potential of agro-industrial residues from the Amazon region to produce activated carbon," *Heliyon*, <https://doi.org/10.1016/j.heliyon.2023.e17189>, 2023.
- [32] A. Preglo, J. Namata, and J. Caculba, "Paracetamol Removal from Aqueous Solution Through Activated Carbon from Mango Seeds," *Chemistry Africa*, vol 6, pp. 699–710, 2023.
- [33] R. Zobia, T. Javid, K. Samia, and A. Ali, "Removal of As(V) and Cr(VI) with Low-Cost Novel Virgin and Iron-Impregnated Banana Peduncle-Activated Carbons," *ACS Omega*, vol. 8, pp. 2098–2111, 2023.
- [34] A. Tarek, K. Uttam, H. Ali, and A. Nurul, "Fruit peel-based mesoporous activated carbon via microwave assisted  $K_2CO_3$  activation: Box Behnken design and desirability function for methylene blue dye adsorption," *International Journal of Phytoremediation*, <https://doi.org/10.1080/15226514.2022.2137102>, 2023.
- [35] S. Bourahla, F. Nemchi, and H. Belayachi, "Removal of the AO7 dye by adsorption on activated carbon based on grape marc: equilibrium, regeneration, and FTIR spectroscopy," *Journal of the Iranian Chemical society*, vol. 20, pp. 669–681, 2023.
- [36] Z. Meijuan, J. Ma, X. Liu, and S. Lili, "Bamboo-Activated Carbon Synthesized by One-Pot Pyrolysis and  $FeCl_2$  Activation for the Removal of Cr(VI) in Aqueous Solutions," *Water*, <https://doi.org/10.3390/w15101891>.
- [37] O. Victor, O. Bello, S. Bello, and A. Samuel, "Removal of 2,4-Dichlorophenol from aqueous medium using activated carbon prepared from cocoa pod husks," *Chemical Data Collections*, <https://doi.org/10.1016/j.cdc.2023.100997>, 2023.
- [38] S. Sedef, K. Mehmet, O. Gulen, and T. Fatima, "Effective Removal of Cationic Dyes from Aqueous Solutions by Using Black Cumin (*Nigella sativa*) Seed Pulp and Biochar," *BioResources*, vol. 18, pp. 3414-3439, 2023.

- [39] M. Affandy, R. Kobun, M. Joseph, H. Kana, "Characterization of activated carbon from waste tea (*Camellia sinensis*) using chemical activation for removal of methylene blue and cadmium ions," *South African Journal of Chemical Engineering*, vol. 44, pp. 113-122, 2023.